Dynamics of driven recurrent networks of ON and OFF cells

Jérémie Lefebvre,[1,*] André Longtin,[1] and Victor G. LeBlanc[2]
[1]*Department of Physics, University of Ottawa, 150 Louis Pasteur, Ottawa, Ontario, Canada K1N 6N5*
[2]*Department of Mathematics and Statistics, University of Ottawa, 585 King Edward Avenue, Ottawa, Ontario, Canada K1N 6N5*
(Received 11 November 2008; revised manuscript received 26 August 2009; published 9 October 2009)

A globally coupled network of ON and OFF cells is studied using neural field theory. ON cells increase their activity when the amplitude of an external stimulus increases, while OFF cells do the opposite given the same stimulus. Theory predicts that, without input, multiple transitions to oscillations can occur depending on feedback delay and the difference between ON and OFF resting states. Static spatial stimuli can induce or suppress global oscillations via a Andronov-Hopf bifurcation. This is the case for either polarity of such stimuli. In contrast, only excitatory inputs can induce or suppress oscillations in an equivalent network built of ON cells only even though oscillations are more prevalent in such systems. Nonmonotonic responses to local stimuli occur where responses lateral to the stimulus switch from excitatory to inhibitory as the input amplitude increases. With local time-periodic forcing, the unforced cells oscillate at twice the driving frequency via full-wave rectification mediated by the feedback. Our results agree with simulations of the neural field model, and further, qualitative agreement is found with the behavior of a network of spiking stochastic integrate-and-fire model neurons.

DOI: 10.1103/PhysRevE.80.041912 PACS number(s): 87.19.lr, 02.30.Ks, 02.50.Ey, 87.19.lp

I. INTRODUCTION

Autonomous and driven responses of networks are a focus of much current research in biological physics. The interplay of feedforward and feedback connections, of both excitatory and inhibitory type, are strong determinants of dynamical behaviors [1,2]. In particular, the modeling of spatially extended neural systems with such connections has received increasing attention as they exhibit a host of interesting dynamical phenomena. Mechanisms have been found for transitions between equilibria and nonhomogeneous states in space and/or in time (see, e.g., [3], and references therein). Propagation and processing delays in biological networks further expand the range of dynamical possibilities [4–6]. Responses to simple localized inputs can lead to localized structures such as bumps and breathers [3,7]. A main challenge lies on modeling responses to static [8] or moving spatial stimuli [9] which are relevant to neural networks. Stochastic spatiotemporal stimuli with varying degrees of spatial correlation, as they occur in naturalistic situations, have also begun to receive attention [10,11]. Another is the inclusion of multiple types of cells, which complicates the bifurcation analysis greatly. For example, two-population systems are under study [3,12–15], where cells in one population have similar properties and connections to other cells.

Sensory systems are a common context in which to model responses of networks to localized spatiotemporal inputs. In many sensory systems however, the cells are divided into ON- and OFF-type cells. The firing rate of an ON (OFF) cell is proportional (inversely proportional) to the amplitude of an external stimulus. The effect of this division on the aforementioned dynamical phenomena has not been studied. ON and OFF cells can similarly drive other cells further along the sensory pathway, but external input to OFF cells is inverted (e.g., by interneurons) in comparison to ON cells. For example, ON (OFF) pyramidal cells (also called *E* and *I* cells, respectively) in the electrosensory lateral line (ELL) lobe of weakly electric fish, which provide the prime motivation for our model below, increase (decrease) their firing rate when the electric field at the primary receptors in their receptive field increases (decreases) [16,17]. ON and OFF cells also occur in many other sensory pathways including visual [18], auditory [19] and pain processing pathways [20], where they further shape receptive fields.

All these pathways further involve recurrent connections from higher nuclei back to ON and OFF cells [10,21]. The role of feedback is a major question in neuroscience, and its answer is likely complicated even by most basic ON/OFF cell properties. In particular, oscillatory activity has been reported in the ELL when there is sufficient spatial correlation in stimuli. This is thought [10,11] to be important for categorical coding, where spatially correlated stimuli are caused by the presence of other fish (and oscillations ensue) while spatially uncorrelated stimuli relate more to prey (and oscillations do not ensue). It has further been shown [22] that such gamma-range oscillations enhance the directional sensitivity of neurons in the electrosensory system. Since very few lateral connections exist within ELL, the interplay between rhythmic activity and recurrent signals from higher nuclei back to ELL is of prime importance to understand how such inputs generate oscillations. As this component of feedback circuitry is part of many senses, our analysis provides a picture of the dynamical effects that can be attributed to this basic skeleton of those sensory systems, as opposed to other pieces of circuitry specific to different senses, such as local connections.

Thus our analysis on driven recurrent networks of ON and OFF cells is particularly motivated by experiments in electroreception, where an increase in the spatial correlation of a stimulus causes oscillatory firing activity, an effect requiring feedback and successfully modeled using ON cells only without local connectivity [10,11]. The fact that OFF cells

*jlefe076@uottawa.ca

are equally involved means that an increase in stimulation does not necessarily increase the feedback signal since ON and OFF cells respond in opposite directions to that input. This raises the question of whether transitions between fixed points and oscillations can still occur and what specific dynamical effects this arrangement might lead to. Our results below show that transitions to oscillatory activity for constant inputs can indeed occur when both ON and OFF cells are present. Further, we predict the paradoxical autonomous and driven responses of delayed feedback networks of ON and OFF cells.

II. MODEL

We focus on the simplest case of a one-dimensional (1D) layer of intercalated ON and OFF cells. We follow the basic connectivity scheme of the electrosensory system, in which each cell, regardless of type, is coupled identically to every other cell via global delayed feedback [16]. This feedback is provided in reality by a distant population to which the ON and OFF cells project; we assume for simplicity that this population sustains the same activity without further processing and feeds it back to all cells in the 1D layer. Since the delayed coupling connectivity is all to all, there is no spatial dimension in the autonomous model. However, the spatial stimulus will impose a spatial dimension, i.e., a topology. Our analysis quantifies how opposing responses of these populations to spatiotemporal input $I(x,t)$ affects activity patterns in the ON-OFF layer. The mean somatic membrane potentials or "activities" $u_{on}(x,t)$ and $u_{off}(x,t)$ obey

$$\hat{D}_{on}u_{on}(x,t) = A(t-\tau) + I(x,t),$$

$$\hat{D}_{off}u_{off}(x,t) = A(t-\tau) + V_o - I(x,t), \tag{1}$$

where $\hat{D}_j = (1 + a_j^{-1}\partial_t)$ with synaptic response time a_j^{-1}. $V_o \in \mathbb{R}$ sets the asymmetry between ON and OFF spontaneous rates. ON and OFF cells produce the same feedback (strength and polarity) to all cells [10]. This global delayed feedback which acts at "3" in Fig. 1 is

$$A(t-\tau) = k\int_\Omega dy\{\alpha_{on}f_{on}[u_{on}(y,t-\tau)] + \alpha_{off}f_{off}[u_{off}(y,t-\tau)]\},$$

where, for j=ON, OFF,

$$f_j(u) \equiv (1 + e^{-\beta(u-h_j)})^{-1} \tag{2}$$

is the firing rate function with threshold h_j and gain β. The finite spatial domain is Ω, while α_j is the relative proportion of j type cells in the population. The delay $\tau > 0$ accounts for processing and axonal conduction times. We set $k=1$ for excitatory and $k=-1$ for inhibitory feedback. Specific ON/OFF neural systems will deviate more or less from this generic configuration, but understanding their driven recurrent dynamics requires first analyzing this generic case. Further elaborations on this basic circuitry, such as the presence of local connectivity seen in other senses, are briefly discussed below.

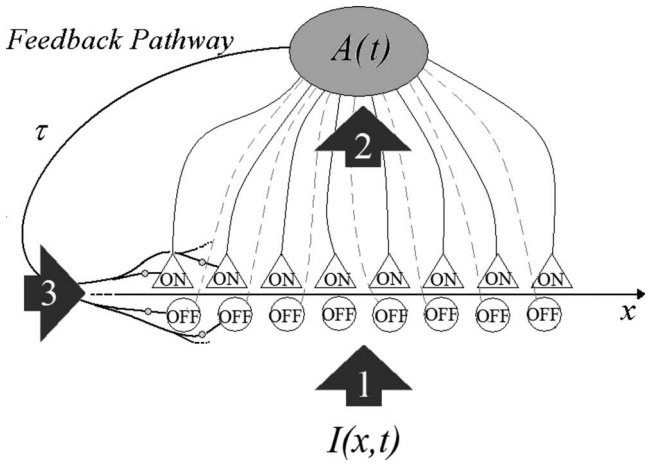

FIG. 1. Sensory processing with feedback. (1) For simplicity, ON cells receive external input $I(x,t)$ directly; OFF cells are identical but receive inverted input via an interneuron (not shown). Apart from feedback, there are no connections between neighboring or distant cells, inspired from the architecture on the electrosensory lateral line lobe. (2) ON/OFF activity projects to higher brain. (3) The summed activity $A(t)$ drives ON/OFF cells after a delay τ.

III. STEADY-STATE ANALYSIS

To set the stage, we examine the case where, with $I(x,t)=0$ and no feedback, ON units do not fire ($\bar{u}_{on} \approx 0$) while OFF units do ($\bar{u}_{off} \approx V_o$). This can be adjusted with V_o to suit specific systems. Note however that this information on V_o is difficult to obtain *in vivo* since the observed firing rate is a combination of the spontaneous activity of the cell and the feedback onto this cell from all cells. The spontaneous rate can be obtained in certain experiments if the feedback can be turned off, e.g., either surgically or pharmacologically, and this "open-loop" knowledge will help calibrate the neural model by adjusting its bias V_o.

The asymmetry V_o plays an important role, seen by performing a bifurcation analysis of (1) in the (β,h) parameter space, as well as a function of the delay τ, for the homogeneous and autonomous case $I(x,t)=0$. Solutions of Eq. (1) are spatially uniform and implicitly determined by

$$\bar{u}_{on} = k\frac{\Omega}{2}[f(\bar{u}_{on}) + f(\bar{u}_{off})],$$

$$\bar{u}_{off} = k\frac{\Omega}{2}[f(\bar{u}_{on}) + f(\bar{u}_{off})] + V_o. \tag{3}$$

For simplicity, we chose $\alpha_{on}=\alpha_{off}=1/2$, $a_{on}=a_{off}=1$, and $h_{on}=h_{off}\equiv h$ so that we may write the firing rate functions f without subscripts.

A. Excitatory feedback $k=1$

For excitatory feedback $k=1$, no oscillatory solutions are possible. In this case, for $V_o=0$, varying β passed the value $4/\Omega$ causes a supercritical pitchfork bifurcation only when $\bar{u}_{on}=\bar{u}_{off}=h=\Omega/2$. Otherwise, if $h \neq \Omega/2$, saddle-node bifurcations occur. The dynamics are thus organized around a

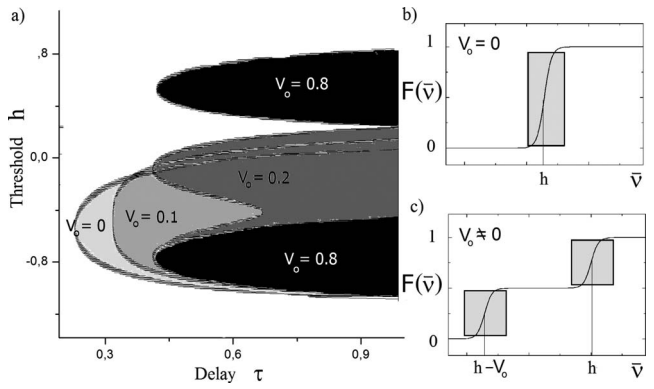

FIG. 2. Oscillatory regimes in the threshold-delay parameter space. Shaded regions, delimited by instability curves, correspond to global temporal oscillations. The shape of these regions is changed by the asymmetry V_o between ON and OFF subpopulations, introducing two effective thresholds in the system [(b)–(c)]; the shaded boxes mark limit cycle behavior. Parameters are $k=-1$, $\beta=25$, $\alpha_j=0.5$, and $\Omega=1$.

cusp point. However, when $V_o\neq 0$ with β fixed, multistability ensues as the activation threshold h is varied, with new fixed points arising via saddle-node bifurcations. We do not analyze this case is greater detail since our main focus below is on inhibitory feedback.

B. Inhibitory feedback $k=-1$

For inhibitory feedback $k=-1$ and for $V_o=0$, the unique fixed point can bifurcate to a stable limit cycle at an appropriate delay [5,6] [see Fig. 2(a)]. Letting $V_o\neq 0$ introduces two distinct instability domains instead of one, as seen in Fig. 2(a) in the $h-\tau$ space. Thus multiple transitions to oscillations are possible. In fact, defining $\bar{u}_{on}=\bar{u}_{off}-V_o\equiv\bar{\nu}$ allows us to recast Eq. (3) more simply as $\bar{\nu}=F(\bar{\nu})\equiv k\frac{\Omega}{2}[f_{on}(\bar{\nu})+f_{off}(\bar{\nu})]$. Thus, $V_o\neq 0$ amounts to introducing two effective thresholds $h_{on}(V_o,I_o=0)=h$ and $h_{off}(V_o,I_o=0)=h-V_o$ [Figs. 2(b) and 2(c)]. The presence of asymmetry $V_o>0$ creates two distinct spontaneous firing rates for ON and OFF populations but does not alter the system threshold per se. This change in variable above is used to represent these different activities by a single state, resulting in a one-dimensional fixed point but which exhibits two "effective" thresholds. The input breaks locally the symmetry introduced by this change in variable and the ON and OFF activities cannot be represented by a single point. From this perspective, plotting stationary firing rate F versus stationary activity $\bar{\nu}$ reveals two distinct regions where oscillations emerge through Hopf bifurcations surrounded by fixed points (plateaus). Steep regions correspond to oscillations of the activity of the ON and OFF population around their respective thresholds h_{on} and h_{off}. Given a fixed point $\bar{\nu}$, each population will respond to input with a different sensitivity and be driven in and out of oscillation by inputs of different amplitude. Oscillations always reach all cells due to feedback.

IV. RESPONSES TO STATIC INPUTS

The results of the last section lay the foundation for understanding how ON and OFF units integrate spatiotemporal signals. From now on, we set $k=-1$ and illustrate responses, first in a regime near the Hopf (large τ) and then in the fixed-point regime (small τ). Stimuli are always applied to ON and OFF cells evenly.

Spatially uniform input $I(x)=I_o$ linearly shifts the steady state defined by Eq. (3). This is equivalent to threshold modifications, $h_{on}=h-I_o$ and $h_{off}=h-V_o+I_o$, such that $h_{on}=h_{off}-V_o+2I_o$. More importantly, a static nonuniform input $I(x,t)=I(x)$ induces in the steady state a nonhomogeneous solution that satisfies

$$\bar{u}_{on}(x)=A(\bar{u}_{on},\bar{u}_{off})+I(x),$$

$$\bar{u}_{off}(x)=\bar{u}_{on}(x)+V_o-2I(x), \tag{4}$$

where we have made the dependence on u_{on} and u_{off} explicit. An input may induce a transition from fixed point to oscillations (Hopf) by moving the variable R across its critical value R_c at the bifurcation defined by

$$\tan[\omega(R_c)\tau]+\omega(R_c)=0 \tag{5}$$

for $\omega(R)=\sqrt{R^2-1}$ where $R=\{\alpha_{on}\int_\Omega dy f'[\bar{u}_{on}(y)]+\alpha_{off}\int_\Omega dy f'[\bar{u}_{off}(y)]\}$; if $|R|>1$, $\omega(R)$ corresponds to the frequency at the bifurcation. The network allows the transition from fixed point to global oscillation as a response to an input of sufficient amplitude. Transition to oscillatory behavior is caused by local units approaching the neighborhood of the feedback activation threshold h represented by the shaded area in Figs. 2(b) and 2(c), leading to higher values of the variable R.

Figure 3(a) demonstrates the effect of the amplitude of a pulse on the variable R defined above. The pulse is a piecewise homogeneous signal that has an amplitude of I_o over a spatial width $\Delta=|x_2-x_1|$ but is set to 0 elsewhere. For $I_o=0$, R sits in a local minima for which $R<R_c$ and ON and OFF populations have stationary firing rates. When a localized input drives the system, R increases as the locally excited units approach the activity level h.

Figure 3(b) illustrates the activity increase in both ON and OFF subunits for some stimulated site located at $x=y$ with respect to the activation curve f, in the spirit of Figs. 2(b) and 2(c). Figure 3(c) illustrates the same for ON units only. In each case, the stimulated ON population increases its activity toward the threshold, resulting in an increase in the value of R. According to this picture, if the pulse amplitude is high enough, the curve $R(I_o)$ crosses the critical value defined by Eq. (5) and oscillatory activity appears throughout the network. Note that if the pulse amplitude increases further, the value of R decreases. Thus, if the pulse amplitude is too high, no oscillatory response will be seen.

Our analysis also reveals that oscillations are less prevalent in an ON/OFF system compared to one with ON cells exclusively (labeled thereafter as ON/ON), in the sense that they occur over a smaller volume of pulse amplitudes and widths. This can be seen in Fig. 3(a) by the larger area occupied by the curve above the critical line $R=R_c$ in the ON/ON case compared to the ON/OFF case. Further, ON/OFF nets can exhibit oscillations for either positive or negative inputs. As one can see in Fig. 3(a), the ON/OFF network allows R to cross the instability threshold R_c for both positive

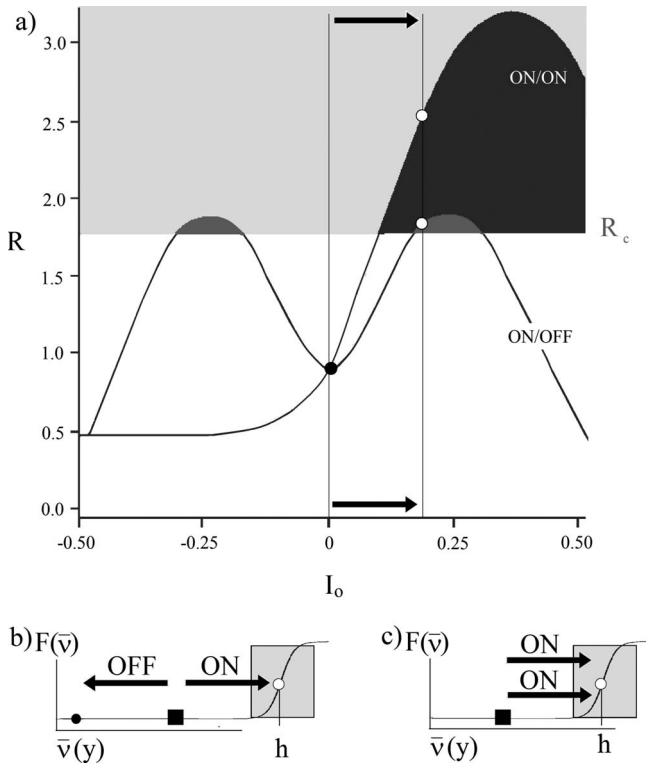

FIG. 3. Impact of local stimulation. (a) Variable R as a function of a localized pulse amplitude. The amplitude of the pulse is I_o over a spatial width of $\Delta=0.6$ and is zero otherwise. Increasing the amplitude will cause the value of R to change, for a network made of equal numbers of ON and OFF cells (ON/OFF) and one built uniquely of ON cells (denoted by ON/ON). In both cases, crossing the critical value R_c causes a Andronov-Hopf bifurcation and the resulting limit cycle becomes stable. Other parameters are $V_o=0.0$, $h=0.1$, $\beta=25$, and $\alpha_j=0.5$. (b) Schematic of local effects of excitatory stimulation in the activity for some driven site $x=y$ in a ON/OFF network. In this example, prior to the input, both ON and OFF units have the same activity denoted by the dark square. Local inputs shift activity states toward (respectively, away from) the threshold h for the case of ON units (respectively, OFF) units. Changes in the variable R, and thus the resulting oscillations, are essentially due here to the change in activity of the ON cells (open circle) since the activity of the OFF cells is negligible (dark circle). (c) Similar behavior occurs in a ON/ON network, but the activities simultaneously approach the threshold, resulting in a greater increase in R, as shown in part (a). The opposite occurs for inhibitory pulses.

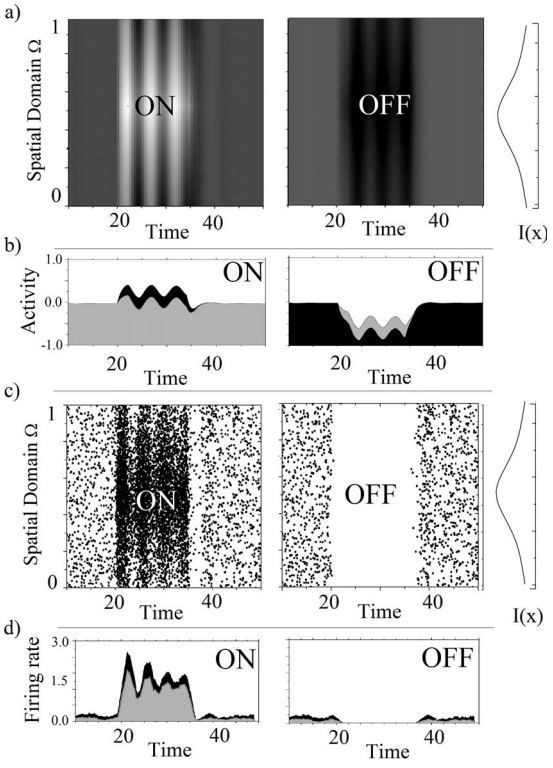

FIG. 4. Oscillatory response triggered by a static input bump. ON (left) and OFF (right) populations responding to a localized positive bump. Gray shading encodes relative activity amplitudes. (b) Central (black) and lateral (gray) response of ON and OFF populations, showing the time evolution of the solutions inside and outside the pulse. The input triggers oscillations from stationary activity states. Parameters are $V_o=0.0$, $\tau=1.8$, $h=0.12$, $\beta=25$, and $\alpha_j=0.5$. The bump has an amplitude $I_o=0.6$ for $t\in[20,35]$, and is set at 0 otherwise. (c) Equivalent phenomenon in a stochastic spiking network of $N=1000$ integrate-and-fire neurons equally spaced on the spatial interval [0,1]. ON cells demonstrate oscillatory firing rates, while OFF cells are inhibited in the subthreshold regime. Parameters are $V_o=0$, $\alpha_j=0.5$, $\tau=1.8$, $D=2.0$, and $h_{on}=h_{off}=1$, with $\mu=0.2$ and $g=-0.05$. The refractory period is $\tau_{ref}=0.1$. The membrane and synaptic time constants are $a=\tau_m=1$. The input amplitude is 2.0 for $20<t<35$ and 0 otherwise. The bump length scale is set at $\sigma=0.6$. (d) Mean firing rate variations in time of ON and OFF cells from LIF simulations. Changes in the cell mean firing rate are shown both inside (black) and outside (gray) the bump. Mean firing rate is stationary prior to stimulation. The bump triggers global firing rate oscillations. A time window of ten integrating steps was taken to approximate the frequencies. Note that time, here and in the following figures, is in arbitrary units which can be mapped to physiological time scales. The firing rate is expressed in spike/τ_m.

and negative pulse amplitudes, while the ON/ON network only does so for positive amplitudes. This result is intuitively expected given the distinct rectification properties of ON and OFF cells.

Interestingly, for some parameters, global oscillations are stable for $I(x)=0$, and the reverse transition is observed, as shown in Fig. 5. We emphasize that distinct ON and OFF populations allow such an instability to occur even if their effective thresholds are not identical. Furthermore, letting an input spatial profile tend to a constant recovers the homogeneous problem described by asymmetry-induced instabilities as in Fig. 2, where limit cycles are only allowed in restricted regions of the $[h(V_o,I_o),\tau]$ parameter space.

A. Numerical simulations

We numerically test these predictions using spatially localized bump stimuli which are biophysically relevant. In Figs. 4 and 5 we consider the response of Eq. (1) to $I(x,t)=I_o(2\sigma)^{-1}\exp[-|x-x_o|\sigma^{-1}]$ if $t_1<t<t_2$ and 0 elsewhere. In Fig. 4, the bump drives the sensory layer for $t>t_1$, and stationary activities lose their stability when the variable R satisfies Eq. (5). Global oscillations appear across the network,

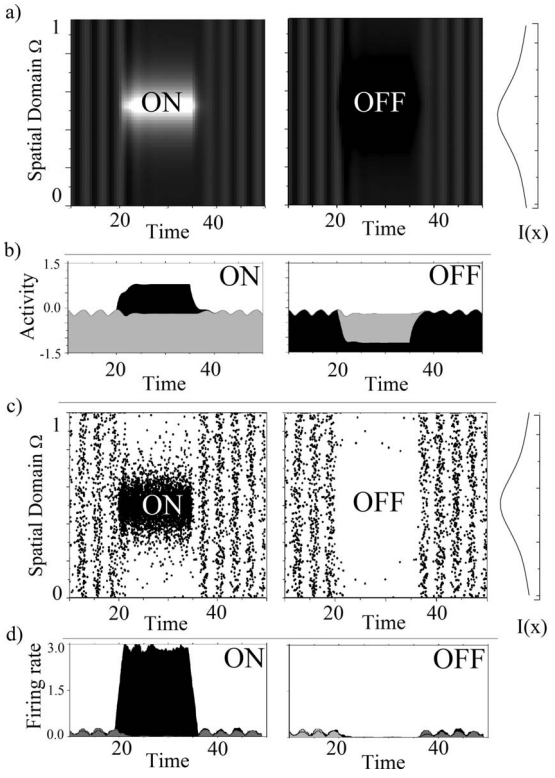

FIG. 5. Bump-shaped stimulus removing global oscillations. (a) As in Fig. 5, ON (left) and OFF (right) cells responses to a localized positive bump are shown. (b) Central (black) and lateral (gray) dynamics shows the damping of the oscillations as the input is turned on. Parameters are $V_o=0.0$, $\tau=1.1$, $h=-0.05$, $\beta=25$, and $\alpha_j=0.5$. The bump has an amplitude $I_o=0.2$ for $t\in[20,35]$, and is set at 0 otherwise. The bump length scale is set here at $\sigma=0.1$. (c) Equivalent phenomenon in a stochastic spiking network of $N=1000$ integrate-and-fire neurons equally spaced on the spatial interval [0,1]. Other parameters are $V_o=0$, $\alpha_j=0.5$, $\tau=1.1$, $D=1.0$, $h_{on}=h_{off}=1$, and $\tau_{ref}=0.1$ with $\mu=0.8$ and $g=-0.06$. The membrane and synaptic time constants are $a=\tau_m=1$. The input amplitude is 0.5 for $20<t<35$ and 0 otherwise. (d) Mean firing rate as a function of time for both ON and OFF cells, inside (black) and outside (gray) the input bump. A time window of ten integrating steps was taken here as well. The firing rate is expressed in spike/τ_m.

modulating the structure of the bump-shaped responses. The reverse mechanism occurs at $t=t_2$ when the bump disappears, and where ON and OFF stationary activities recover their stable fixed-point behavior. In Fig. 5(a), the opposite phenomenon is observed. Prior to the bump, limit cycles are stable for the chosen parameters until $t=t_1$. The global equilibrium [Eq. (4)] becomes stable during the input and loses stability at input offset as the boundary defined by Eq. (5) is crossed again.

This behavior is further qualitatively reproduced in simulations of noisy spiking networks of leaky-integrate-and-fire neurons (LIF) with all-to-all coupling. Our aim is to show that a simple generic form of this model adapted to the ON/OFF context can show qualitatively similar behavior to that of the neural field model. Our goal is not to provide a detailed representation of experimental data nor a detailed correspondence between the LIF and the neural field formulation. The respective ON and OFF membrane potentials v_j^{on} and v_j^{off} in a population of N cells obey

$$\tau_m \frac{dv_j^{on}}{dt} = -v_j^{on} + g\sum_{t_i} \eta(t_i-\tau) + \mu + \xi(t) + I(j,t),$$

$$\tau_m \frac{dv_j^{off}}{dt} = -v_j^{off} + g\sum_{t_i} \eta(t_i-\tau) + \mu + \xi(t) + V_o - I(j,t),$$

with Gaussian white noise $\xi(t)$ of intensity D, feedback gain g, spiking times of all neurons $\{t_i\}$ and bias current μ. The synaptic response function is given by $\eta(s)=ae^{-as}$ whenever $s>0$ and zero otherwise. The synaptic time constant a is here set to 1. The membrane time constant τ_m is also fixed to 1. The asymmetry V_o and input amplitude I_o must be tuned in order to reach the appropriate membrane potential correspondence between the neural field and LIF formulations of network dynamics. Indeed, our numerical experiments suggest that a close relationship exists between both model formulations, but its full determination is not the aim of the current work. Figure 5(b) shows the firing rate oscillations vanish across the domain as the input is turned on. The input causes the feedback to reach a critical amplitude, bringing cells subthreshold and thus inhibiting network activity. Pyramidal cells in the electrosensory system can increase their firing rates more than tenfold in response to a stimulus so large variations are physiological. The specific mean firing rates observed in our simulations, as well as the frequency of the emerging firing rate oscillation via the Hopf bifurcation, are consequences of the specific choices of the synaptic time constant (set throughout to $a=1$) as well as the membrane time constant (set throughout to $\tau_m=1$) and the delay. For example, lower firing rate oscillation frequencies are observed for larger delay values (not shown). If time units are scaled such that 1 (time unit)=10 ms, as the physiologically relevant delay range suggests, one obtains firing rate oscillation frequencies around 50 Hz, as observed in experimental studies on the electrosensory system [10,11,23].

B. Central and lateral responses

We next consider network responses to input for smaller delays, i.e., in the fixed-point regime. For $V_o\neq 0$, the response to a local pulse, where $I(x,t)=I_o$ for $x\in[x_1,x_2]$ if $t_o<t<t_1$ and $I_o=0$ otherwise, might alter feedback in nonintuitive ways. Indeed, asymmetry between ON and OFF populations induces, lateral to the pulse, a nonmonotonic response as I_o increases [Fig. 6(a)]. As input increases, the contribution of the stimulated cells to the global feedback is first reduced, then enhanced. The behavior of both ON and OFF cells shown in Figs. 7(a) and 7(b) illustrates the phenomenon in Figs. 6(a) and 6(b). For a small pulse, the magnitude of global feedback drops: lateral activity goes up. For a larger pulse, ON activity increases further, OFF activity remains low as for the small pulse, and global feedback is stronger: lateral activity is now less than before the pulse. This is a consequence of the feedback component $A(t)$ varying nonmonotonically with respect to I_o, which is reflected

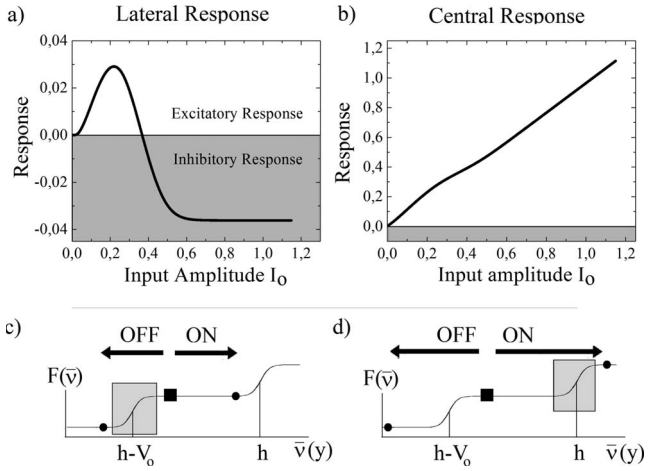

FIG. 6. Response vs I_o outside the pulse is nonmonotonic. Inhibitory feedback decreases, as OFF activity massively decreases, but then increases, as ON cells are locally recruited by the pulse and continue to increase their rate. Note that the magnitude of the response depends on the choice of parameters, especially the feedback gain $|k|$ (here set to 1), but is smaller than that in the central response. (b) Response vs I_o inside the pulse (central ON cell) is monotonic but with two slopes. The same nonmonotonic feedback effect as in (a) occurs but is compensated by I_o. The difference between the curves in (a) and (b) is simply I_o. Note that for central OFF cells, the response curve is monotonically decreasing, due to the inhibitory effect of the incoming pulse. The pulse amplitude is I_o for $x \in [0.35, 0.75]$ and $t \in [20, 25]$, and 0 otherwise, $V_o=0.3$, $h=0.05$, $\beta=25$, $\tau=0.2$, and $\alpha_j=0.5$, with random initial conditions. (c) Schematic description of local effects of stimulation for some driven site $x=y$, resulting in nonmonotonic lateral response. The variable used here is $\bar{v}$ in order to represent the asymmetrical solutions u_{on} and u_{off} by a single state with two distinct thresholds. Given the parameters considered, the fixed point $\bar{v}=F(\bar{v})$ before the pulse (dark square) is located in the plateau between $h_{off}=h-V_o$ and $h_{on}=h$ but closer to h_{off}. By analogy to the initial formulation (i.e., without $\bar{v}$), the stimulation puts u_{onf} and u_{off} in different parts of the response curve. As the input drives the units, the activity of the OFF cells (dark circle to the left) is inhibited and crosses the threshold h_{off}, while ON cells (dark circle to the right) are not excited sufficiently to reach their response threshold h_{on}. The cumulative effect across all stimulated sites generates a decrease in the amplitude of the inhibitory feedback and lateral activity increases. (d) As the input amplitude increases further, the activity of the ON cells crosses h_{on} and augments the amplitude of the inhibitory feedback, leading to a lateral decrease in activity.

by the lateral response behavior plotted in Fig. 6(a). The magnitude of this effect depends on the choice of parameters, especially the feedback gain, which can be adjusted to amplify the excitatory and inhibitory responses. The central response will, however, always be more important than the lateral response. This phenomenon is also observed in our integrate-and-fire network, where the lateral firing rate first increases then decreases when the input amplitude is augmented, as shown in Fig. 8. We further note that excitatory feedback ($k=+1$) alone brings solutions away from the threshold; response curves are monotonic. Small excitatory feedback in parallel with dominant inhibitory feedback is equivalent to a small change in the gain k, as long as solutions maintain their stability properties for $k<0$ (not shown).

V. RESPONSE TO TIME-PERIODIC STIMULI

More paradoxical effects are seen in the fixed-point regime with stimuli of the form $I(x,t)=I(x)\sin(\omega_o t)$, where $2\pi/\omega_o$ is large compared to the synaptic $(1/a_j)$ and feedback (τ) time scales. For a local pulse $I(x)=I_o$ for $x \in [x_1, x_2]$ and $I(x)=0$ elsewhere, we observe a lateral discrepancy in the dominant frequencies of the population activity (Fig. 9). Interestingly, this is a spatial change in oscillatory mode, but without any space dependent connectivity. The feedback integrates input from both ON $[+I(x,t)]$ and OFF $[V_o-I(x,t)]$ cell populations which, for periodic input, are in antiphase. Given the form of the firing rate function, each of these feedback components is roughly a half-wave-rectified version of the input oscillating at frequency ω_o. The sum of these two components produces a feedback that fulfills the role of a second forcing term, driving the system globally at frequency $2w_o$ as a full-wave rectified version of the input. This rhythm always appears regardless of whether the periodic pulse drive is local or global. However, inside the pulse, the direct input competes with the feedback, producing a dominant rhythm at ω_o for sufficiently large I_o. Outside the pulse, only the global feedback-driven rhythm at $2\omega_o$ is seen.

Further, near to the Hopf regime (e.g., for larger delays), a time-periodic pulse of large amplitude and/or spatial extent will induce a sequence of Hopf bifurcations as the condition in Eq. (5) is cyclically fulfilled. The result is a complex waveform that includes bursts relating to the Hopf-induced limit cycles (not shown). Their analysis will be presented elsewhere.

VI. DISCUSSION

We have performed a bifurcation analysis of a neural field of ON and OFF cells with all-to-all delayed coupling. For excitatory coupling we have found multistability between homogeneous fixed-point states. Paradoxical effects are predicted to occur in such networks with inhibitory coupling, on which we have put more emphasis. Our work was directly inspired by the configuration of the electrosensory system in which local connections are weak compared to delayed feedback connections. Localized inputs near the Hopf regime can turn oscillations on or off. Compared to equivalent networks made fully of ON cells, we have shown that such nets exhibit transitions to oscillations over a narrower range of parameters that characterize the pulse input—namely, its width and strength. However, the ON/OFF network is shown to exhibit such transitions for both stimulus polarities. Our work supports the observation of oscillations in the electrosensory system seen with spatially correlated inputs [10,11] when both ON and OFF cells are present. A next step is to extend our analysis to stochastic spatiotemporal stimuli to show how, as in those studies, the spatial correlation of a stochastic input can bring on gamma-range oscillations and whether the Hopf curve behaves as shown here for localized pulse inputs.

In the fixed-point regime, localized inputs produce monotonic or nonmonotonic input-output relations. Local time-

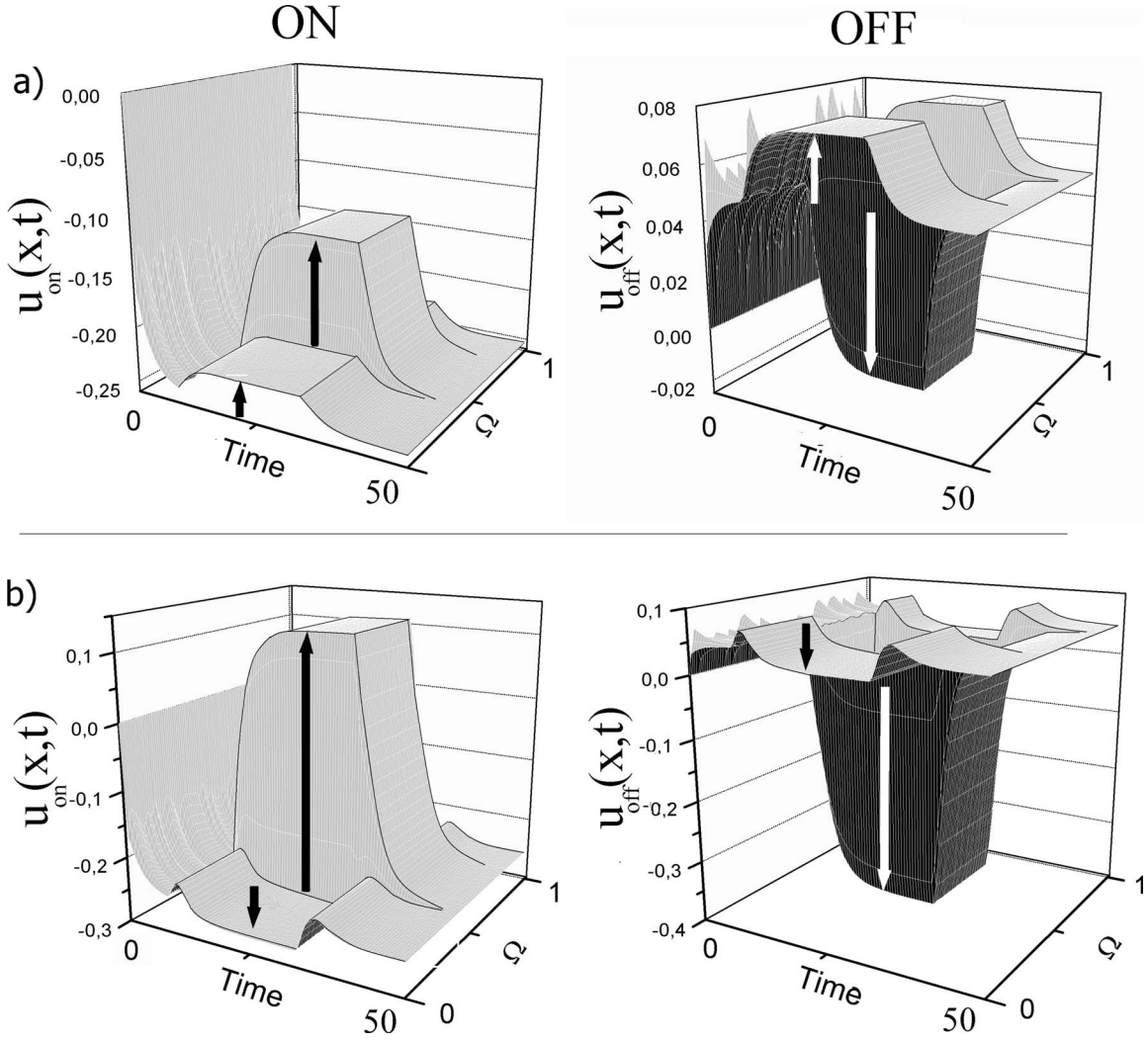

FIG. 7. Response of the ON and OFF cells to a localized discontinuous pulse of amplitude I_o in the fixed-point regime. Here, for $I_o=0$, OFF cells are firing and ON cells are almost silent. The initial decay seen in the time course of the ON cells is caused by this choice of initial conditions. (a) ON (left) and OFF (right) populations activity in response to the pulse. Here $I_o=0.1<V_o$. Activity of all cells increases. (b) The pulse amplitude is increased to $I_o=0.4>V_o$; lateral activity now decreases. The pulse is identical as in Fig. 6.

periodic forcing leads to coexisting network oscillations at different frequencies in the sense that we can see one gamma frequency centrally, where cells are in the receptive field of primary receptors (such as electroreceptors projecting to ELL) receiving the pulse stimulation, while another frequency is measured laterally to the pulse. In fact, experiments have been proposed [24] to measure these nonmonotonic lateral as well as frequency doubling effects, especially to see the spread in the range of gamma frequencies that ensues.

Another direction of interest is to consider how local connectivity interacts with the global delayed loop considered here. Our results are qualitatively and numerically unchanged (not shown) if nondelayed inhibitory feedback is also present, mimicking local connectivity. The same is true when moderate positive delayed feedback is present at the same time as the negative all-to-all delayed feedback considered here. A deeper analysis of the dynamical effects caused by such additional circuitry is beyond the scope of our study and is left for future work. Local connectivity makes the system truly spatial to begin with, rather than only in the presence of a stimulus as is the case in the present study.

We note that all-to-all networks of stochastic LIF neurons have been analyzed using a mean field analysis [25] in which the field contributed by all cells affects the mean bias and the noise level of each cell. They have found oscillatory behavior when inhibition is sufficiently strong, which is in line with our findings using neural field theory and with our numerics on the neural field and the LIF's. Because of the all-to-all coupling, including sparse random coupling, their theory is also without space, as is ours. Although we consider only excitatory or inhibitory connections in isolation, our work goes beyond their study by considering that ON and OFF cells both receive external input and respond in opposite directions to it. Further we consider the effects of time-varying inputs. It will be of interest to develop their theory or that in [11] to see how the noise influences the effects that we describe. It will also be of interest to see what are the prime determinants of the oscillation frequency in delayed nets of all-to-all coupled ON and OFF cells as a

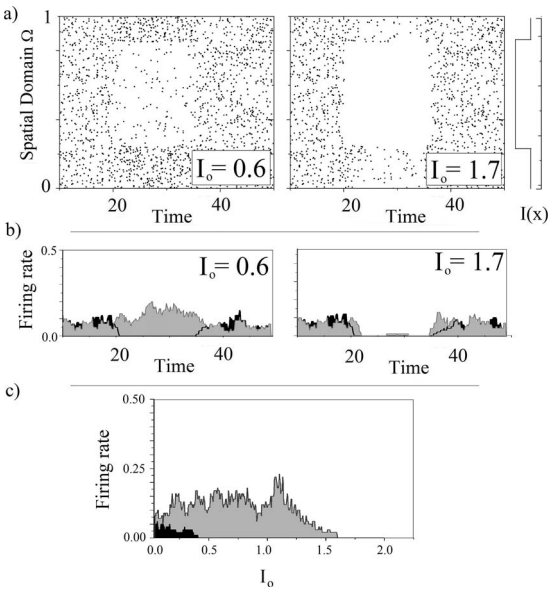

FIG. 8. Nonmonotonic lateral response of OFF cells to a spatially localized pulse in a LIF network. (a) A spike plot of a network of $N=1000$ cells, qualitatively reproducing the results shown in Fig. 6 and 7 is shown. Smaller input amplitudes (left) generate an excitatory lateral response, while the response for larger amplitudes becomes inhibitory (right). (b) Time evolution of the firing rate both inside (black) and outside (gray) the pulse. As the input amplitude increases from 0.6 to 1.7, the lateral response changes from excitatory to inhibitory, and the firing rate first increases and then decreases. (c) Central (black) and lateral (gray) firing rate as a function of the input amplitude I_o, qualitatively reproducing the results shown in Figs. 6(a) and 6(b). The lateral response exhibits the same nonmonotonicity, while the central response is monotonically decreasing, as expected from center OFF cells. Given this parameter set, OFF cells are in the suprathreshold regime due to the choice of a high value of V_o, while the ON cells are maintained in the subthreshold regime where they fire at a very low rate (not shown). The nonmonotonic response of the ON cells can be appreciated in the neural field model (Fig. 7) because the activity is plotted (rather than spike times), and this activity can take values below the threshold. Parameters are $V_o=1.2$, $\alpha_j=0.5$, $\tau=0.1$, $D=1.0$, and $\tau_{ref}=0.1$. $\mu=0.1$, $h=1.0$, and $g=-0.9$. The input has an amplitude of I_o between $[0.25,0.85]$ for $20<t<35$ and zero otherwise. A time window of ten integrating steps was taken to compute the firing rates. The firing rate is expressed in spike/τ_m.

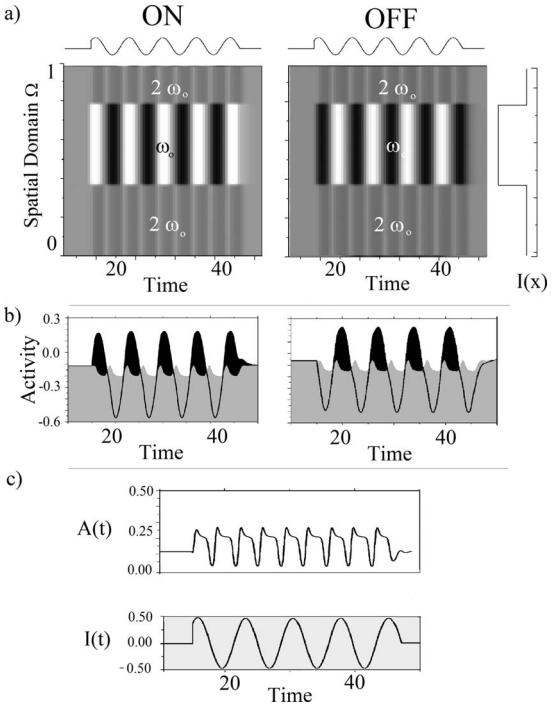

FIG. 9. Lateral frequency doubling effect. (a) Spatially inhomogeneous responses of ON (left) and OFF (right) populations to local periodic forcing with $I_o=0.5$ over the region $x\in[0.35,0.75]$ and zero elsewhere for $15<t<45$. (b) Time evolution of the activity of ON and OFF cells inside (black) and outside (gray) the time-periodic pulse, showing the central-lateral response discrepancy. (c) Associated time evolution of the feedback signal $A(t)$, showing that combined ON and OFF contributions make the recurrent component oscillate at twice the input frequency. Parameters are $\omega_o=0.9$, $V_o=0.05$, $h=0.0$, $\beta=25$, $\tau=0.4$, and $\alpha_j=0.5$.

function of the balance of excitation and inhibition, the noise level, and of the relative time scales of excitatory and inhibitory networks, as has been investigated for autonomous [26] and driven networks [30].

As mentioned in the Introduction, ON and OFF cells are found in most sensory pathways and in conjunction with feedback. The simple circuit investigated here can thus serve as a stepping stone toward understanding responses to inputs, including the onset of oscillations, in other senses, since the oscillation mechanism discussed here is accessible to these senses. Oscillations in the visual system induced by spatially correlated stimuli have been argued to rely mainly on local circuitry in cortex. Further, locally generated oscillations can be amplified by a recurrent loop such as the thalamocortical loop [21]. This is clearly different from the electrosensory system where the feedback loop is important (see also work on the nucleus isthmi in the visual tectum by Wessel *et al.* [27]) As these resulting temporal oscillations are thought to be of particular significance for higher cognitive functions [28,29], their continued dynamical analysis in the context of more biophysically detailed driven networks of ON and OFF cells is further warranted.

ACKNOWLEDGMENTS

We thank A. Hutt, L. Maler, and W. Nesse for discussions and NSERC Canada and FQRNT for support.

[1] V. M. Eguiluz, D. R. Chialvo, G. A. Cecchi, M. Baliki, and A. V. Apkarian, Phys. Rev. Lett. **94**, 018102 (2005).
[2] M. N. Artyomov *et al.*, Proc. Natl. Acad. Sci. U.S.A. **104**, 18958 (2007).
[3] C. Laing and S. Coombes, Network **17**, 151 (2006).
[4] M. Dhamala, V. K. Jirsa, and M. Ding, Phys. Rev. Lett. **92**, 074104 (2004).
[5] S. A. Campbell *et al.*, J. Dyn. Differ. Equ. **7**, 213 (1995).
[6] A. Roxin, N. Brunel, and D. Hansel, Phys. Rev. Lett. **94**, 238103 (2005).
[7] D. Pinto and B. Ermentrout, SIAM J. Appl. Math. **62**, 226 (2001).
[8] P. C. Bressloff, S. E. Folias, A. Prat, and Y. X. Li, Phys. Rev. Lett. **91**, 178101 (2003).
[9] S. E. Folias and P. Bressloff, SIAM J. Appl. Math. **65**, 2067 (2005).
[10] B. Doiron *et al.*, Nature (London) **421**, 539 (2003).
[11] B. Doiron, B. Lindner, A. Longtin, L. Maler, and J. Bastian, Phys. Rev. Lett. **93**, 048101 (2004).
[12] H. R. Wilson and J. D. Cowan, Biophys. J. **12**, 1 (1972).
[13] P. Blomquist *et al.*, Physica D **206**, 180 (2005).
[14] D. Golomb and G. B. Ermentrout, Phys. Rev. Lett. **86**, 4179 (2001).
[15] B. Vladimirski *et al.*, J. Comput. Neurosci. **25**, 39 (2008).
[16] N. J. Berman and L. Maler, J. Exp. Biol. **202**, 1243 (1999).
[17] F. Gabbiani, Network Comput. Neural Syst. **7**, 61 (1996).
[18] E. R. Kandel and J. H. Schwarz, *Principles of Neural Science* (Elsevier, New York, 1983).
[19] D. A. Robin and F. L. Royer, J. Acoust. Soc. Am. **82**, 1207 (1987).
[20] H. L. Fields *et al.*, J. Neurophysiol. **74**, 1742 (1995).
[21] D. Lumer *et al.*, Cereb. Cortex **7**, 207 (1997).
[22] J. U. Ramcharitar, E. W. Tan, and E. S. Fortune, J. Neurophysiol. **96**, 2319 (2006).
[23] B. Lindner, B. Doiron, and A. Longtin, Phys. Rev. E **72**, 061919 (2005).
[24] L. Maler (private communication).
[25] N. Brunel and V. Hakim, Neural Comput. **11**, 1621 (1999).
[26] N. Brunel and X.-J. Wang, J. Neurophysiol. **90**, 415 (2003).
[27] U. Meyer *et al.*, Biol. Cybern. **99**, 79 (2008).
[28] D. L. Wang, Neural Networks **12**, 579 (1999).
[29] C. Borgers *et al.*, Proc. Natl. Acad. Sci. U.S.A. **105**, 18023 (2008).
[30] M. J. Chacron, A. Longtin, and L. Maler, Phys. Rev. E **72**, 051917 (2005).